Master's Thesis of Department of Brain and Cognitive Sciences

Aberrant hyperfocusing for non-target as indicated by elevated theta phase-gamma amplitude coupling in schizophrenia

조현병에서 세타 위상-감마 진폭 결합 증가로
나타나는 비표적 자극에 대한 비정상적인 과집중

August 2023

Graduate School of Seoul National University
Department of Brain and Cognitive Sciences

Su-Jin An

Aberrant hyperfocusing for non-target as indicated by elevated theta phase-gamma amplitude coupling in schizophrenia

Advisor: Jun Soo Kwon, Sang-Ah Lee

Submitting a master's thesis of
Department of Brain and Cognitive Sciences

August 2023

Graduate School of Brain and Cognitive Science
Seoul National University

Su-Jin An

Confirming the master's thesis written by
Su-Jin An

August 2023

Chair 이 인 아 (Seal)

Vice Chair 권 준 수 (Seal)

Examiner Lee Sang Ah (Seal)

Abstract

Background: Selective attention is an important cognitive domain underlying cognitive symptom in patients with schizophrenia (SCZ). Damage to brain oscillations may contribute to cognitive impairment, and theta phase-gamma amplitude coupling has been demonstrated to be involved in sensory processing, attention, and working memory. This study aimed to investigate electroencephalographic marker for aberrant hyperfocusing, a novel framework for impaired selective attention, using theta phase-gamma amplitude coupling (TGC) in patients with SCZ.

Methods: Fifty-four patients with SCZ and 73 healthy controls (HCs) participated in electroencephalographic recording during auditory oddball paradigm. For each non-target and target condition, TGC was calculated using the source signals from the 25 brain regions of interest (ROIs) related to attention networks and sensory processing and compared across the groups and conditions using two-way analysis of covariance. Relationship of altered TGC with the performances on the trail making test, type A and B (TMT-A/B) were explored.

Result: Patients with SCZ showed elevated TGC in left inferior frontal gyrus (IFG) and superior temporal gyrus (STG) in non-target condition compared to HCs. There was no group difference in target condition. Correlation analyses revealed that TGC in left IFG was positively correlated with reaction time of TMT-A/B.

Conclusions: Aberrant hyperfocusing for non-target condition as reflected by elevated TGC in attention related brain regions were related to behavioral performances on the TMT-A/B in patients with SCZ. This study suggests that TGC can be an electrophysiological marker for aberrant hyperfocusing of attentional processing that may

result in cognitive impairments in patients with SCZ.

Keyword: Hyperfocusing, Cross-frequency coupling (CFC), Theta phase-gamma amplitude coupling (TGC), Auditory oddball task, Electroencephalography (EEG), Event-related potential (ERP)

Student Number: 2021-21614

Table of Contents

Chapter 1. Introduction

1.1. The importance of selective attention in schizophrenia

Patients with schizophrenia (SCZ) is classified as a cognitive disorder because the cognitive symptoms first appear early in the illness and have an important impact on the progression and prognosis of positive and negative symptoms (Kahn & Keefe, 2013; Ueoka et al., 2011). Cognitive impairments reported in patients with SCZ appear to be extended and moderate to severe in various domains such as attention, working memory, verbal learning and memory, and executive functions (Bowie & Harvey, 2006). Among the many cognitive domains that reported to be impaired in patients with SCZ, of particular interest is selective attention. It regulates other higher cognitive processes and symptoms, so knowing the mechanisms of selective attention is essential for understanding cognitive symptom in patients with SCZ (Daniel H. Mathalon et al., 2004; Fan & Posner, 2004; Galaverna et al., 2012).

Despite the presence of impaired selective attention in patients with SCZ, they sometimes show normal attentional functioning (Beck et al., 2016; Gold et al., 2006). It can be explained by aberrant hyperfocusing hypothesis, which is a new framework to explain impaired selective attention in patients with SCZ and other psychiatric disorders (Ashinoff & Abu-Akel, 2021; Luck et al., 2014). Aberrant hyperfocusing refers to excessive concentration on broad range of stimuli or tasks rather than specific goal, which directly affect simple selective attention and can further affect higher-order cognitive functioning such as flexible thinking (Luck et al., 2019). This phenomenon is not due to general cognitive impairment or lack of motivation but rather an abnormal level of

attention towards specific activities (Luck et al., 2019).

1.2. Brain oscillation and cognition

As the moment-by-moment integration within and between brain regions is considered important as a mechanism for the functioning of many cognitive domains (Wang et al., 2021), brain oscillation can be an important marker to identify these temporal dynamics (Friston, 1998; Uhlhaas et al., 2008). Brain oscillations refer to rhythmic electrical activity in the brain that is thought to underlie various cognitive processes, including attention (Herrmann et al., 2016). Different types of brain oscillations have been linked to different functions (Hirano & Uhlhaas, 2021). For example, theta oscillations (frequency band: 4-7 Hz) are associated with working memory and top-down control (Haciahmet et al., 2021; Riddle et al., 2020), while gamma oscillations (frequency band: > 30 Hz) are associated with sensory processing and attention (Balz et al., 2016; Mathalon & Sohal, 2015).

In patients with SCZ, dysfunctional brain oscillation may result in deficient coherence between cognition and behavior leading to the typical symptoms and cognitive deficits (Hirano & Uhlhaas, 2021; Uhlhaas & Singer, 2010). Disrupted oscillatory activity particularly in the theta and gamma frequency ranges has been associated with impaired selective attention in patients with SCZ, but these result are still inconsistent and have not yet established (Basar & Guntekin, 2013; Lynn & Sponheim, 2016; Shin et al., 2011). Overall, the relationship between impaired selective attention and brain oscillations is still an area of active research in patients with SCZ. Further studies are needed to understand the neural mechanisms underlying aberrant hyperfocusing and to determine whether

targeting brain oscillations may be a way for treating cognitive deficits in patients with SCZ.

1.3. Theta phase-gamma amplitude coupling

How attention is impaired for each single frequency band has been extensively studied in patients with SCZ, but existing studies have mainly focused on a single frequency band (Basar & Guntekin, 2008; Hirano & Uhlhaas, 2021; Javitt et al., 2020). Cross-frequency coupling has emerged as a new approach for investigating cognitive function in the brain, suggesting that groups of neurons oscillating at varying frequencies engage with one another to construct nested assemblies rather than relying solely on a single frequency band (Canolty et al., 2006; Canolty & Knight, 2010; Palva et al., 2005; Tort et al., 2010).

High-frequency gamma oscillations and low-frequency theta oscillations play distinct roles in representing information in the brain. While gamma oscillations are responsible for encoding individual pieces of information, theta oscillations provide the neurophysiological basis for the temporal intervals during which these items are represented. The interaction between theta and gamma oscillation, referred to as theta-gamma coupling, is essential for organizing the sequence of these items within a specific time frame (Lisman & Jensen, 2013; Rajji et al., 2017; Tort et al., 2010). In particular, it is known that the phase of theta in the low-frequency band controls the amplitude of gamma in the high-frequency band, which is called theta-gamma coupling (TGC) (Colgin, 2015; Lisman & Buzsaki, 2008; Lisman & Jensen, 2013). Numerous studies conducted on humans have demonstrated that TGC serves as a marker for cognitive functioning. Specifically, it has been associated with various cognitive processes including sensory

information processing, attention, and working memory (Brooks et al., 2020; Papaioannou et al., 2022; Park et al., 2013).

In patients with SCZ, decreased TGC has been reported while performing rather complex working memory or executive function tasks, supporting that TGC can be an electrophysiological marker for higher-order cognitive dysfunction in patients with SCZ (Barr et al., 2017; Popov et al., 2015). In resting-state, patients with SCZ showed abnormally elevated TGC in default mode network related brain areas, in line with the previous findings that patients with SCZ have dysfunctions in allocation of cognitive resources to prepare for successful cognitive execution (Lee et al., 2020; Sheffield & Barch, 2016). However, previous studies on TGC during cognitive task performances reported decreased TGC which doesn't fit for aberrant hyperfocusing hypothesis for patients with SCZ (Barr et al., 2017; Popov et al., 2015). This may be because they used higher-order cognitive tasks such as working memory or executive function tests which are too complex for assessing aberrant hyperfocusing in attentional processing. Rather simple attentional task such as oddball task should be investigated to reveal neural correlate of aberrant hyperfocusing in selective attentional processing of patients with SCZ.

1.4. Auditory oddball task for aberrant hyperfocusing

The auditory oddball task is a suitable paradigm for aberrant hyperfocusing in patients with SCZ. During this task, participants listen to a sequence of auditory stimuli, with the majority of condition being the same "non-target" sound and occasional rare "target" sounds. This task has been widely studied as it can predict the progression of patients with SCZ into a chronic state (Hamilton et al., 2019) and is used as an indicator of overall

functioning and symptom (Kim et al., 2018; Shim et al., 2014). In addition, considering that patients with SCZ showed elevated TGC in resting-state where they are in preparation state for future cognitive task performing state (Kim et al., 2022; Lee et al., 2020), aberrant hyperfocusing may be prominent while in preparation state during non-target stimuli rather than during executing responses to target stimuli in patients with SCZ.

Previous studies have confirmed TGC impairment only at the scalp-level measure, and the brain regions where the scalp-level damage originated in patients with SCZ have not been identified. The auditory oddball task is not a task involving a single area, but is closely related to two large attentional networks consisting of the dorsal and ventral (Kim, 2014): the dorsal attentional network, which comprises the frontal eye field (FEF), inferior frontal junction (IFJ), located in the posterior extent of the inferior frontal sulcus, superior parietal lobule (SPL), medial intraparietal sulcus (IPS) and motion-sensitive middle temporal area (MT1). Ventral attentional network, which comprises the temporoparietal junction (TPJ), anterior insula (AI), and adjacent frontal operculum (FO) and the anterior cingulate cortex (ACC). Sensory regions are reported to be damaged in patients with SCZ when performing the oddball task (Kiehl & Liddle, 2001), this brain regions need to be combined to understand the neural mechanism of aberrant hyperfocusing in this disease.

1.5. Aims and hypothesis

We aimed to investigate electrophysiological marker of aberrant hyperfocusing in patients with SCZ by examining TGC during both non-target and target stimuli while performing an auditory oddball task in brain regions related to attention networks and sensory processing.

We hypothesized that patients with SCZ will show elevated TGC during non-target stimuli in line with previous TGC studies and aberrant hyperfocusing hypothesis. In addition, we explored correlation of elevated TGC and behavioral performances on Trail Making Test, Type A and B (TMT-A/B) which measures attention, processing speed, and executive functioning.

Chapter 2. Method

2.1. Participant

A total of 54 patients of SCZ and 73 healthy controls (HCs) participated in this study. Patients of SCZ were recruited from the inpatient and outpatient clinic of the Department of Neuropsychiatry at the Seoul National University Hospital (SNUH). The patients were diagnosed with schizophrenia using the Structured Interview for the Diagnostic and Statistical Manual of Mental Disorders, Fourth Edition Axis I Disorders (SCID-I). The severity of clinical symptoms and general functional status were assessed using the Positive and Negative Syndrome Scale (PANSS) and the Global Assessment of Functioning (GAF) scale, respectively, by experienced psychiatrists. The recruitment of HCs was conducted via internet advertisement. Potential HCs were excluded when they had a past or present diagnosis of any psychiatric disorders and had any first- to third-degree relatives suffering from psychotic disorders. Common exclusion criteria for both patients of SCZ and HCs included a history of substance abuse or dependency (except for nicotine), severe head trauma or neurological disease, severe medical illness, sensory impairments, or intellectual disability (Intelligence Quotient [IQ] < 70). This study was conducted in accordance with the Declaration of Helsinki and was approved by the Institutional Review Board of SNUH. All study participants fully understood the study procedures and provided written informed consent (IRB no. H-1110-009-380).

2.2. Task paradigm

Acoustic stimuli were presented using tubular insert earphones with the STIM2 system (Neuroscan, E1 Paso, TX). The study involved three experimental blocks, each comprising a pseudo-random arrangement of 50-millisecond (80 dB, 10 ms rise/fall) tones that varied in frequency. The target stimuli occurred infrequently at a rate of 18% (180/1000), with the frequency set at 1500 Hz, while the non-target stimuli occurred frequently at an incidence rate of 82% (820/1000), with the frequency set at 1000 Hz. Participants were directed to push a button once they detected the rare target sound. The inter-stimulus interval was 1300ms. Task paradigm was show in Figure 1.

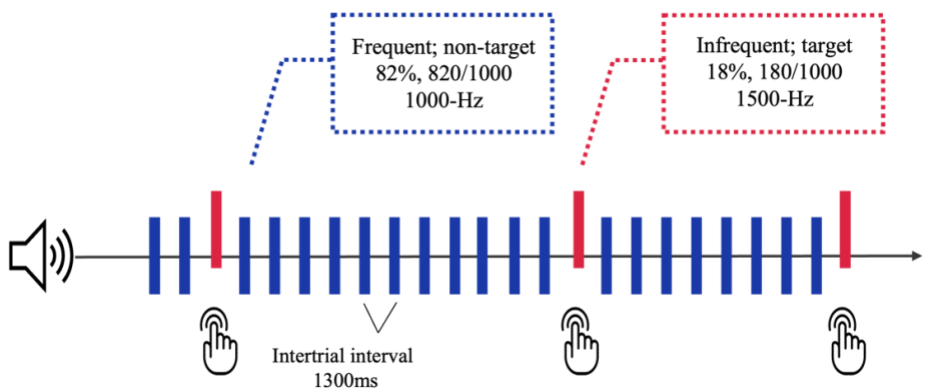

Figure 1. Auditory oddball paradigm task paradigm

2.3. Data acquisition and measurement

Continuous electroencephalographic (EEG) recording was acquired using a Neuroscan 128-Channel Synamps system with 64 scalp electrodes based on the 10–20 international system. Electrodes at each mastoid site served as reference electrodes. The EEG signals were digitized at a rate of 1000 Hz and filtered analogously between

frequencies ranging from 0.05 Hz to 100 Hz. Eye-movement artifacts were detected via recording horizontal and vertical electrooculograms using electrodes situated below and on the outer canthus of the left eye. All electrode sites demonstrated resistance levels that fell under or equal to 5 kΩ during data acquisition procedures.

EEG data preprocessing and analysis were performed using MATLAB R2021b (Mathworks, Natick, MA, USA) and EEGLAB toolbox (Delorme & Makeig, 2004). EEG data were down-sampled to 500 Hz and filtered 0.1 Hz high-pass filter. To eliminate high-amplitude artifacts, a data cleaning procedure was performed, and the rejected channels were interpolated up to 10%. Data were re-referenced to a common average reference. Data were epoched between 100 ms prestimulus and 900 ms poststimulus and the baseline was corrected using mean amplitude during 100 ms before stimulus onset. Independent component analysis (ICA) was executed, following which the SASICA toolbox and visual examination were utilized to identify and eliminate any ocular artifacts and electrocardiographic components (Chaumon et al., 2015).

The P300 amplitude and latency for target condition were identified using a peak detection method which identifies the most positive deflection point between 250 and 450 ms poststimulus at 3 centro-parietal electrode sites (Cz, CPz, and Pz). Three electrodes were selected as P300 (P3b) shows maximal amplitude in the parietal area (Hsu et al., 2021). The N100 amplitude and latency for non-target condition were identified using a peak detection method which identifies the most negative deflection point between 50 and 200 ms poststimulus at 3 frontal-central electrode sites (Fz, FCz, and Cz). Three electrodes were selected as N100 (N1) shows minimal amplitude in the parietal area (Duncan et al., 2022).

2.4. Spectral analysis for MGFP and Source analysis for TGC

Epochs were concatenated to 5000 ms (± 150 ms) according to previous studies that the length of data affects the MI value (Barr et al., 2017; Rajji et al., 2017; Voytek et al., 2013). For target stimuli, data was recorded from stimulus onset until button response whereas for non-target stimuli, only data up until 300 ms after stimulus onset was used. All epoch selections were randomized and checked whether there is another artifact or not.

MGFP was calculated to check the spectral power of the concantenated data prior to source analysis. To perform spectral analysis, the concatenated data underwent fast Fourier transformation using a Hamming window resulting in EEG spectral power values measured in μV^2 ranging between 1-49 Hz for each electrode site analyzed. MGFP was computed as the average sum of all EEG spectral powers acquired from every frequency at each of the 62 electrodes utilized during recording sessions using arithmetic mean calculations. To determine the power of theta (4-7 Hz) and gamma (30-49 Hz), we calculated the power of these bands separately.

For analyzing the EEG source, the concatenated data for each condition was used in the LORETA-KEY alpha software program and standardized low resolution electromagnetic tomography (sLORETA) (Pascual-Marqui, 2002). Based on the meta-analysis (Kim, 2014), 25 regions of interest (ROIs) which are related to auditory oddball task were selected using the Broadman area (BA), which areas show in Table 1 and Figure 2. From each ROI's centroid voxel, theta and gamma range signals were extracted through a basic finite impulse response filter implemented in EEGLAB.

Table 1. Montreal Neurological Institute (MNI) coordinates of centroid voxel in each Brodmann area (BA) related to auditory oddball task.

MNI			Lobe	Structure	BA
X	Y	Z			(Brodmann Area)
-30	-5	55	Frontal	Middle Frontal Gyrus	BA 6
-20	-65	50	Parietal	Precuneus	BA 7
-30	30	35	Frontal	Middle Frontal Gyrus	BA 9
-35	20	0	Sub-lobar	Insula	BA 13
-15	-85	0	Occipital	Lingual Gyrus	BA 17
-55	-25	5	Temporal	Superior Temporal Gyrus	BA 41
-5	30	20	Limbic	Anterior Cingulate	BA 24
-40	15	-30	Temporal	Superior Temporal Gyrus	BA 38
-50	-40	40	Parietal	Inferior Parietal Lobule	BA 40
-45	-30	10	Temporal	Transverse Temporal Gyrus	BA 41
-60	-10	15	Temporal	Transverse Temporal Gyrus	BA 42
-30	25	-15	Frontal	Inferior Frontal Gyrus	BA 47
50	-30	45	Parietal	Inferior Parietal Lobule	BA 40
30	-5	55	Frontal	Middle Frontal Gyrus	BA 6
15	-65	50	Parietal	Precuneus	BA 7
30	30	35	Frontal	Middle Frontal Gyrus	BA 9
35	15	-5	Sub-lobar	Insula	BA 13
15	-85	0	Occipital	Lingual Gyrus	BA 17
55	-20	5	Temporal	Superior Temporal Gyrus	BA 41
5	30	20	Limbic	Anterior Cingulate	BA 24
40	15	-30	Temporal	Superior Temporal Gyrus	BA 38
50	-45	45	Parietal	Inferior Parietal Lobule	BA 40
45	-30	10	Temporal	Transverse Temporal Gyrus	BA 41
60	-10	15	Temporal	Transverse Temporal Gyrus	BA 42
30	25	-15	Frontal	Inferior Frontal Gyrus	BA 47

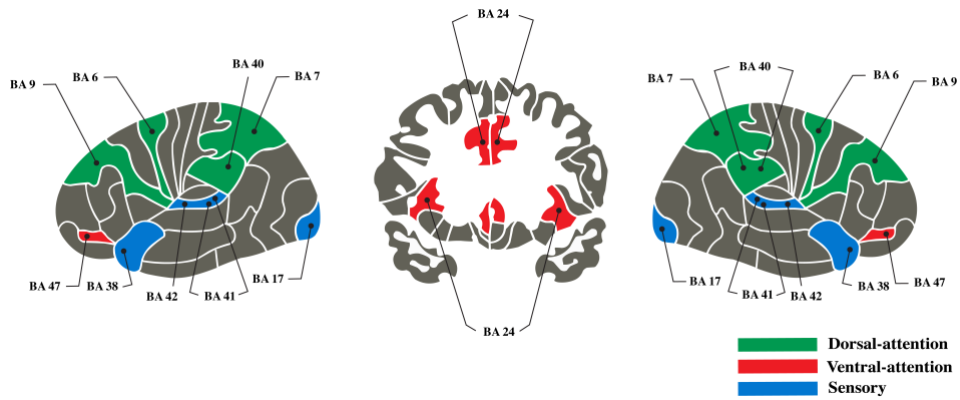

Figure 2. Regions of interest related to auditory oddball task were selected using the Broadman area (BA). L, Left; R, Right.

The modulation index (MI) for TGC was analyzed based on filtered data (Tort et al., 2010). To calculate MI, the hilbert transform was used to obtain the phase of the theta band and the amplitude of the gamma band. The phase of the theta band was divided into 18 bins with a range of 20 degrees, and the average of the gamma band amplitudes corresponding to each bin was calculated. Permutation tests were performed on the individual concatenated data to verify that significant TGC MI was present within each of the selected 25 ROIs. For the permutation test, each theta phase and gamma amplitude data of 5000 ms (± 150 ms) obtained from randomly selected epochs in each ROI were randomly matched on 1000 iterations, and the MI distribution was calculated. The permutation result revealed that TGC MI value of the 25 ROIs were significantly greater than randomly obtained TGC MI value in all subjects, so it is considered as the actual TGC MI value. All processing steps of this study are summarized in Figure 3.

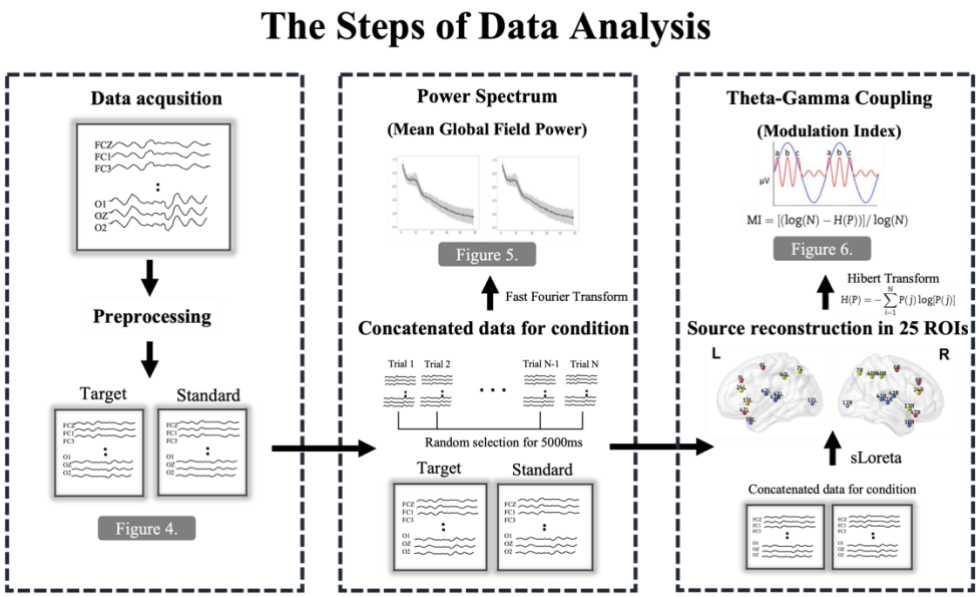

Figure 3. Flowchart diagram of the steps of data analysis.

2.5. Statistic analysis

Statistical analysis was performed using R (v4.1.2; R Core Team 2021) and MATLAB R2021b (Mathworks, Natick, MA, USA). Independent samples t-tests were used to determine between-group differences in age, behavioral data, and TMT-A and TMT-B reaction time. For the comparison of categorical data such as sex and handedness, a chi-square test was conducted. In all group comparison analyses, age and sex were used as covariates. Before performing group comparison, we winsorized the data by replacing the lower and upper 1% of the data with the 10th and 90th percentile values, respectively (Hill et al., 2020; Mueller et al., 2011). 2-way mixed analysis of covariance (ANCOVA) was performed using the between-subject factor of group (i.e., HCs, patients with SCZ), the within-subject factor of electrode site (i.e., non-target: Fz, FCz, Cz, target: Cz, CPz, Pz)

per condition to assess group difference in P3b and N1 amplitude and latency. 2-way mixed ANCOVA was also performed several times using the between-subject factor of group (i.e., HCs, patients with SCZ), the within-subject factor of condition (i.e., target, non-target) to assess group difference in MFGP and TGC MI values. If Mauchly's sphericity test was violated, Greenhouse-Geisser correction was employed. False discovery rate (FDR) correction was applied to correct for multiple comparisons in all group comparison. Pearson's correlation analysis was performed to investigate the relationship between the altered TGC MI values and TMT-A/B reaction time in schizophrenia patients. False discovery rate (FDR) correction was applied to correct for multiple comparisons in all group comparison and correlation analyses. All p-values below 0.05 were considered significant for all statistical analyses.

Chapter 3. Result

3.1. Characteristics of the participants

Table 2 summarizes the demographic and clinical characteristics of the participants. No group difference was identified in gender, handedness, education, and behavioral performances on auditory oddball task between patients with SCZ and HCs. However, patients with SCZ were older ($t = -5.874$, $P < 0.005$), had lower IQ ($t = 3.118$, $P < 0.05$), and had slower reaction time ($t = -5.482$, $P < 0.005$) to the target stimuli than HCs. Patients with SCZ also showed longer reaction time in TMT-A ($t = -5.161$, $P < 0.005$) and TMT-B ($t = -5.792$, $P < 0.005$) compared to HCs.

Table 2. Demographic and clinical characteristics and cognitive function tests.

	Healthy controls	Patients with SCZ	Statistical analysis [a]	
	(n = 73)	(n = 54)	T or $\chi 2$	P
Demographic characteristics				
Age (years) [b]	23.611 (4.369)	30.750 (7.938)	-5.874	<0.005 **
Sex (male/female)	38/33	35/19	1.180	0.278
Handedness (right/left)	62/6	34/5	2.140	0.343
IQ [c]	112.152 (11.367)	103.750 (14.563)	3.118	<0.05 *
Education (years) [d]	14.250 (1.670)	14.020 (2.527)	0.559	0.577
DOI (months) [e]	-	126.559 (73.420)		
Behavior Data				
Error rate (%)	2.832 (4.786)	4.631 (7.267)	-1.582	0.117

Reaction Time (sec)	337.947 (75.950)	429.136 (103.297)	-5.482	<0.005 **
Cognitive function test				
Reaction time in TMT [d]				
TMT-A (sec)	22.787 (7.462)	34.444 (13.773)	-5.161	<0.005 **
TMT-B (sec)	54.714 (15.602)	100.467 (51.396)	-5.792	<0.005 **
Clinical characteristics				
PANSS [e]				
Total	-	66.298 (17.831)		
Positive symptom	-	17.106 (6.647)		
Negative symptom	-	17.149 (6.065)		
General symptom	-	32.043 (8.366)		
GAF [f]	-	47.632 (10.173)		
Prescribed medication [g]				
Antipsychotics	-	54 (100)		
Antidepressants	-	5 (9.259)		
Mood stabilizers	-	13 (24.074)		
Benzodiazepines	-	21 (38.888)		

Abbreviations: IQ, intelligent quotient; TMT – A, trail marking test, part A; TMT – B, trail marking test, part B, DOI, duration of illness; PANSS, Positive and Negative Syndrome Scale; GAF, Global Assessment of Functioning

The values are presented as the mean (standard deviation).

a. Independent samples t-test; chi-square test for categorical data.

b. Data were missing from 1 healthy control and 2 patients with SCZ.

c. Data were missing from 7 healthy controls and 14 patients with SCZ.

d. Data were missing from 5 healthy control and 4 patients with SCZ.

e. Data were missing from 7 patients with SCZ.

f. Data were missing from 9 patients with SCZ.

g. Number (percentage) of subjects who were prescribed each medication at the time of electroencephalography (EEG) measurement.

* Statistical significance is at $p < 0.05$.

** Statistical significance is at $p < 0.005$.

3.2. ERP amplitude and latency for each condition

Figure 4(a) shows the grand averaged P300 waveforms per condition. Figure 4(b) illustrates topographic maps of the P300 amplitudes of the HC and SCZ participants per condition.

For the target condition, there were a significant main effect of group ($F = 24.338$, $P < 0.005$) and the main effect of electrode site ($F = 7.079$, $P < 0.005$) on the P3b amplitude. A significant interaction effect of group x electrode site was observed ($F = 27.789$, $P < 0.005$). Post hoc revealed CPz amplitude ($F = 26.1$, $P_{FDR} < 0.005$) and Pz amplitude ($F = 55.1$, $P_{FDR} < 0.005$) were smaller in patients with SCZ compared to HCs. In terms of the P3b latency, no significant main effect of electrode site ($F = 2.261$, $P = 0.118$) and interaction effect of group x electrode site ($F = 2.959$, $P = 0.066$) were observed, but the significant main effect of group ($F = 4.751$, $P = 0.030$) was present.

For the non-target condition, there was a significant main effect of group ($F = 33.413$, $P < 0.001$), but there were no significant main effect of electrode site ($F = 0.601$, $P = 0.439$) and interaction effect of group x electrode site ($F = 2.906$, $P = 0.089$) on the N1 amplitude. In terms of the N1 latency, no significant main effect of group and interaction effect of group x electrode site ($F = 2.959$, $P = 0.066$) were observed, but the main effect of electrode site ($F = 4.073$, $P = 0.045$) was significant.

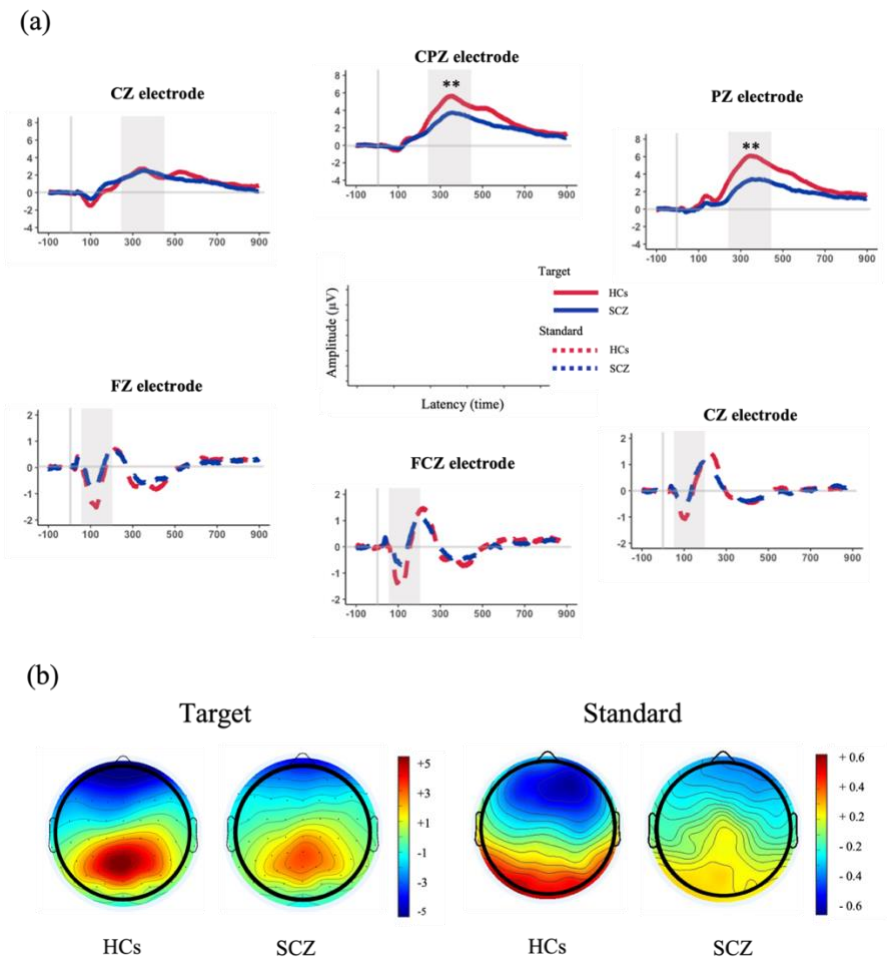

Figure 4. (a) Grand-averaged P300 waveforms of the target at Cz, CPz, and Pz between groups and Grand-averaged N100 waveforms of the non-target at Fz, FCz, and Cz between groups. (b) Two-dimensional P300 topographic maps of the target between groups and N100 topographic maps of the non-target between groups. The grey shading indicates the time window for finding the peak in each condition. The double asterisk symbol (**) indicates that the statistical significance of the amplitude is FDR-corrected $p < 0.005$.

3.3. MGFP spectral analysis for each condition

Figure 5(a) shows the MGFP spectral power for 1-49 Hz compared between groups by condition. Figure 5(b) shows a comparison of power in the theta-band range (4-7 Hz) between groups, and Figure 5(c) shows a comparison of power in the gamma-band range (30-49 Hz) between groups.

For theta power, there were a significant main effect of group ($F = 24.338$, $P_{FDR} = 0.028$) and interaction effect of group x condition ($F = 5.292$, $P_{FDR} = 0.046$), but no significant main effect of condition ($F = 0.393$, $P = 0.532$) on theta power. Post hoc analyses revealed theta power of the non-target condition ($F = 10.8$, $P_{FDR} = 0.002$) were larger in patients with SCZ compared to HCs. For gamma power, there was no significant main effect of group ($F = 0.063$, $P = 0.803$) and condition ($F = 0.049$, $P = 0.825$), and interaction effect of group x condition ($F = 0.052$, $P = 0.820$).

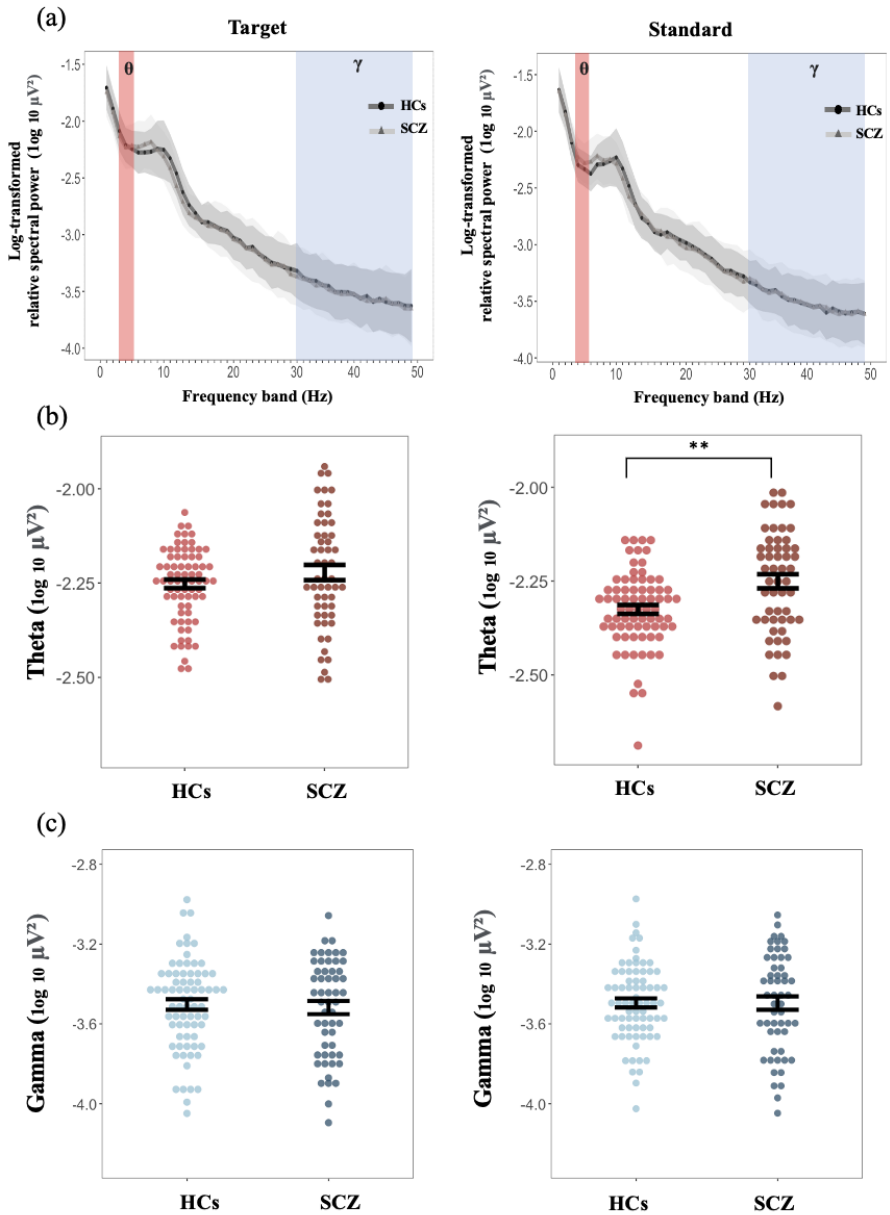

Figure 5. (a) A comparison of the power spectrum of patients with SCZ and HCs per condition. The shading (black and grey) on the graph represents the standard deviation, with the red shading showing the range of the theta band and the blue shading showing the range of the gamma band. **(b) The comparison of theta power for each condition. (c) The comparison of gamma power for each condition. All figures are for target on the left and non-target on the right.** The horizontal and vertical lines in the group indicate the mean and standard deviation of band power. The double asterisk symbol (**) indicates that the statistical significance is FDR-corrected $p < 0.005$.

3.4. TGC MI analysis for each condition

TGC MI results are presented in Table 3 and Figure 6. The detailed two-way ANCOVA results of TGC MI values in 25 cortical ROIs between patients with SCZ and HCs are provided in Table S1. Two-way ANCOVA with the diagnostic group as between-subject factors (i.e., patients with SCZ, HCs), condition as within-subject factors (i.e., non-target, target), and age and sex as covariates revealed a significant group by condition interaction in left inferior frontal gyrus (IFG; $F = 12.537$, $P_{FDR} = 0.007$) and superior temporal gyrus (STG; $F = 13.458$, $P_{FDR} = 0.009$). There was no significant main effect of group nor condition in those ROIs. To find specific group or condition which contributed group by condition interactions, we performed ANCOVA with age and sex as covariates for post-hoc analysis. Group comparison of TGC MI values in each condition revealed that TGC MI values in the left IFG ($F = 5.960$, $P_{FDR} = 0.032$) and STG ($F = 13.800$, $P_{FDR} < 0.005$) during non-target condition were higher in patients with SCZ compared to HCs. There was no group difference of TGC MI values during the target condition. In addition, comparison of TGC MI values according to conditions in each group showed that patients with SCZ exhibited higher TGC MI values in non-target condition compared to target condition in the left IFG ($F = 19.500$, $P_{FDR} < 0.005$) and STG ($F = 11.000$, $P_{FDR} < 0.005$). There was no difference of TGC MI values according to condition in HC group.

Table 3. Comparison of theta-gamma coupling (TGC) between patients with SCZ and HCs per condition.

	BA	Cortical Region	MNI			TGC MI value		Statistical analysis (P_{FDR}) [a]		
			X	Y	Z	Mean (SD)	Mean (SD)	Df	F	P_{FDR}
						Patients with SCZ	HCs			
Non-target	47L	IFG	-30	25	-15	0.014 (0.007)	0.009 (0.005)	123	5.960	0.032*
	38L	STG	-40	15	-30	0.014 (0.007)	0.009 (0.005)	123	13.800	<0.005**
Target	47L	IFG	-30	25	-15	0.010 (0.005)	0.010 (0.005)	123	2.720	0.135
	38L	STG	-40	15	-30	0.011 (0.005)	0.011 (0.006)	123	0.166	0.684
						Non-target	Target			
Patients with SCZ	47L	IFG	-30	25	-15	0.014 (0.007)	0.010 (0.005)	51	19.500	<0.005**
	38L	STG	-40	15	-30	0.014 (0.007)	0.011 (0.005)	51	11.000	<0.005**
HCs	47L	IFG	-30	25	-15	0.010 (0.005)	0.011 (0.005)	70	1.790	0.186
	38L	STG	-40	15	-30	0.009 (0.005)	0.011 (0.006)	70	3.960	0.067

Abbreviation: BA, Brodmann area; MNI, Montreal Neurological Institute and Hospital; TGC, theta-gamma coupling; MI, modulation index; L, left; R, right; IFG, inferior frontal gyrus; STG, superior temporal gyrus.
The values are presented as the mean (standard deviation).
a. Analysis of covariance with false discovery rate (FDR) correction.
* FDR-corrected p value is at <0.05. **FDR-corrected p value is at <0.005

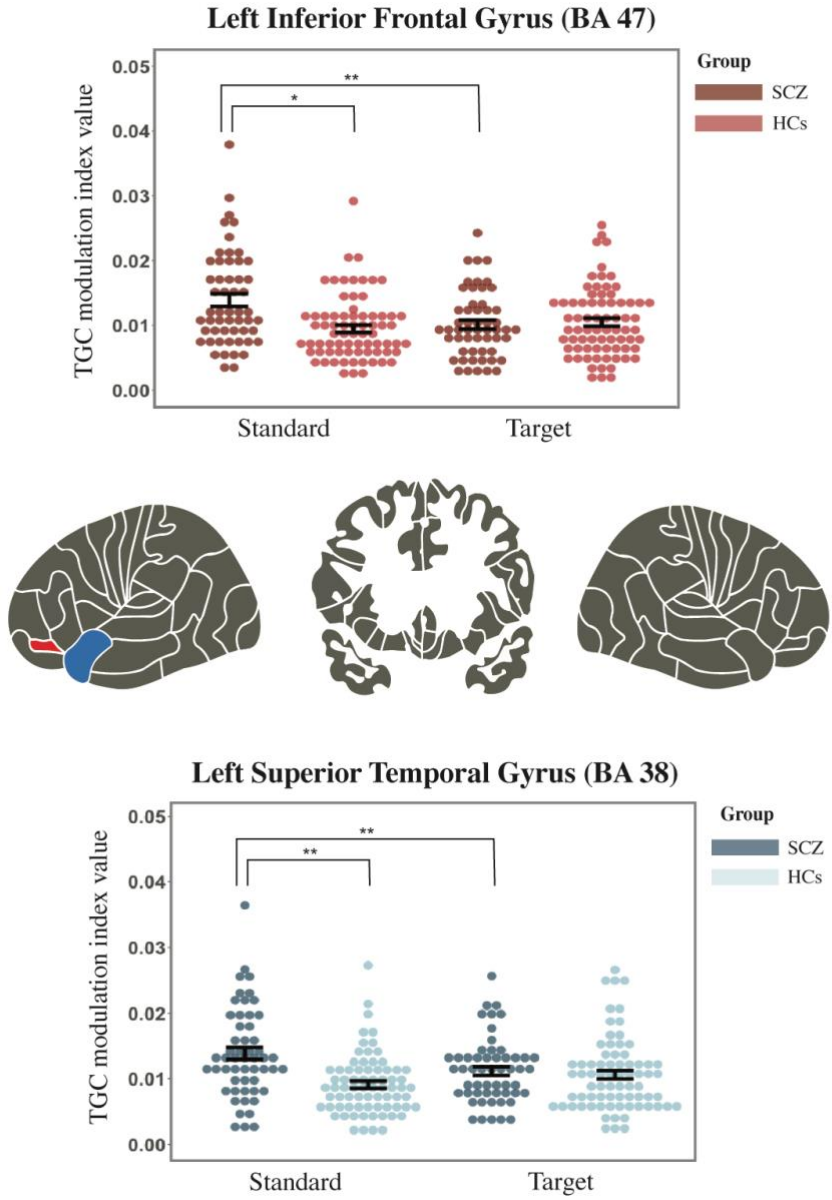

Figure 6. A comparison of the TGC MI values of patients with SCZ and HCs per condition. Each brain region was represented by a Brodmann Area (BA). The horizontal and vertical lines in the group indicate the mean and standard deviation of TGC MI values. Asterisk symbol (*) indicates that the statistical significance is FDR corrected $p < 0.05$. The double asterisk symbol (**) indicates that the statistical signifnce is FDR-corrected $p < 0.005$.

3.5. Correlation between TGC MI value and cognitive functioning

Through Pearson's correlation analysis, we confirmed association of TGC MI values of left STG and IFG, which were significantly higher in patients with SCZ than in HCs, with TMT-A/B reaction time. Pearson's correlation analysis showed that significant association between TGC MI value of left IFG in the non-target condition and reaction time in TMT-A ($R = 0.38$, $P_{FDR} = 0.022$) and TMT-B ($R = 0.45$, $P_{FDR} = 0.006$) in patients with SCZ (Figure 7).

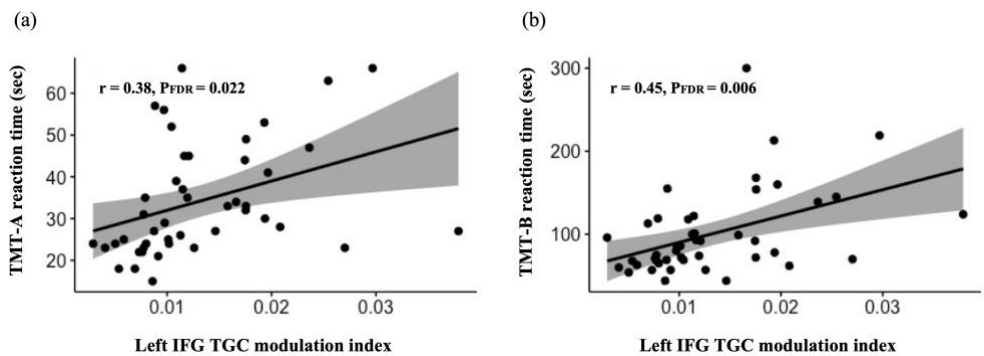

Figure 7. Correlation between the theta phase-gamma amplitude coupling (TGC) of the left inferior frontal gyrus (IFG) and the performance on TMT tests.

Chapter 4. Discussion

4.1. Summary

This study aimed to investigate a neural correlate of aberrant hyperfocusing in patients with SCZ in relationship with cognitive performances by analyzing TGC in brain regions related to attention networks and sensory processing during performing relatively simple auditory oddball task. We found elevated TGC MI values in the left IFG and STG during non-target condition in patients with SCZ compared to HCs. In addition, larger TGC MI values of left IFG and STG were found in non-target condition compared to those in target condition in patients with SCZ, which were not found in HCs. In patients with SCZ, elevated TGC MI values in left IFG were correlated with worse behavioral performance in TMT-A and -B. These results suggest that TGC can be an electrophysiological marker of aberrant hyperfocusing and highlight the role of left IFG in the dysfunctions in cognitive performances affected by aberrant hyperfocusing in patients with SCZ.

4.2. Elevated TGC of non-target condition in patients with SCZ and correlation with other cognition

In this study, TGC MI values in non-target condition were larger in patients with SCZ compared to HCs. In addition, schizophrenia patients showed greater TGC MI values in non-target condition than in target condition, but there was no condition difference found in HCs. These findings are in line with aberrant hyperfocusing hypothesis explaining that patients with SCZ have dysfunctions in controlling the degree of paying attention between less important non-target stimuli and more important target stimuli (Hahn et al., 2020;

Luck et al., 2014; Sawaki et al., 2017). Similarly, resting-state TGC in patients with SCZ was shown to be increased suggesting that the aberrant hyperfocusing presents even in resting-state when paying attention is not needed (Kim et al., 2022; Lee et al., 2020), while studies using rather complex higher-order cognitive tasks such as working memory or executive function tests reported decreased TGC in those patients (Barr et al., 2017; Popov et al., 2015). Because patients with SCZ pay more attention to less important stimuli due to aberrant hyperfocusing than HCs do, they could not use sufficient attentional resources in performing higher-order cognitive tasks reflected by decreased TGC and poor behavioral performances during working memory or executive function tests (Hahn et al., 2022; Luck et al., 2019). The positive correlation between increased TGC MI values in the non-target condition and delayed response time in TMT-A and -B found in this study support this interpretation.

Among the ROIs related with attention networks and sensory processing, elevated TGC MI values during non-target condition in patients with SCZ were found in left IFG and STG. The IFG is important in higher-order cognitive processing such as response inhibition, language processing, and empathic expression (Chavan et al., 2015; Liakakis et al., 2011), and STG plays a role in auditory perception and processing (Golubic et al., 2019; Schroger et al., 2015). Previous functional magnetic resonance imaging (MRI) studies on patients with SCZ reported altered activity in IFG and STG in relationship with dysfunctions in semantic or auditory processing (Gur & Gur, 2010; Mwansisya et al., 2017). In line with previous studies on altered IFG and STG functioning in patients with SCZ, the current study results suggest that left IFG and STG are important in aberrant hyperfocusing in patients with SCZ as reflected by elevated TGC MI values in those regions. In addition,

considering the current study finding that elevated TGC MI values of left IFG in non-target condition were positively correlated with delayed response time in TMT-A and -B performances, left IFG may be more important in aberrant hyperfocusing affecting the behavioral performance of cognitive performances, especially for attention, processing speed, and executive functions.

4.3. Limitation

This study has several limitations. First, the participants in the current study were not matched by age and sex, thus we controlled those variables by using them as covariates in group comparison analysis. Second, we could not use individual structural MRI in source analysis due to limited structural MRI data, which provide detailed structural information about the brain and can be useful for pinpointing the source of EEG signals (Bledowski et al., 2004). However, the high-density EEG system we used can compensate the accuracy of source localization at least in partial (Sohrabpour et al., 2015). Third, most of patients with SCZ participated in this study were taking medications such as antipsychotics or benzodiazepines. Because the relationship between EEG oscillation including TGC and medications remains controversial (Minzenberg et al., 2010; Rosburg et al., 2004) and we found no significant association between the dose of medication and TGC MI values in schizophrenia patients, we did not control medication effect in statistical analysis.

4.4. Conclusion

In conclusion, the current study provides supporting evidence for aberrant hyperfocusing which have been suggested as a mechanism for cognitive dysfunctions in

patients with SCZ. In addition, we suggest that elevated TGC in left IFG and STG can be an electrophysiological marker for aberrant hyperfocusing in patients with SCZ, which can be utilized for future biomarker studies to investigate schizophrenia pathophysiology related to cognitive dysfunctions. Considering that the TGC in the left IFG had significant relationship with behavioral performances in the TMT-A and -B in this study, left IFG may be a target for neuromodulation therapeutics to improve cognitive dysfunctions in patients with SCZ. Future research are needed to further confirm the role of TGC as an electrophysiological marker for aberrant hyperfocusing in schizophrenia pathophysiology and neuromodulation therapeutics.

Table S1. Two-way analysis of covariance (ANCOVA) results of theta phase-gamma amplitude coupling (TGC) modulation index (MI) values in 25 cortical regions of interest (ROIs).

Broadman area (BA)	Cortical ROIs	MNI			Effect	Statistical analysis (P_{FDR}) [a]		
		X	Y	Z		Df	F	P_{FDR}
BA 6L	Middle frontal gyrus	-30	-5	55	Group	123	11.693	**0.021***
					Condition	123	0.137	0.989
					Group * Condition	123	6.673	0.069
BA 7L	Precuneus	-20	-65	50	Group	123	0.818	0.657
					Condition	123	0.218	0.943
					Group * Condition	123	1.113	0.814
BA 9L	Middle frontal gyrus	-30	30	35	Group	123	10.965	**0.013***
					Condition	123	0.302	0.913
					Group * Condition	123	0.185	0.879
BA 13L	Insula	-35	20	0	Group	123	7.416	0.058
					Condition	123	1.056	0.695
					Group * Condition	123	1.238	0.838
BA 17L	Lingual gyrus	-15	-85	0	Group	123	0.815	0.613
					Condition	123	0.585	0.858
					Group * Condition	123	0.376	0.796
BA 41L	Superior temporal gyrus	-55	-25	5	Group	123	4.395	0.136
					Condition	123	0.419	0.927
					Group * Condition	123	0.112	0.839
BA 24L	Anterior cingulate	-5	30	20	Group	123	1.310	0.531
					Condition	123	0.317	0.957
					Group * Condition	123	0.391	0.833
BA 38L	Superior temporal gyrus	-40	15	-30	Group	123	4.496	0.150
					Condition	123	0.013	0.987
					Group * Condition	123	13.458	**0.009***

BA 40L	Inferior parietal lobule	-50	-40	40	Group	123	2.761	0.275
					Condition	123	2.173	0.894
					Group * Condition	123	0.184	0.836
BA 41L	Transverse temporal gyrus	-45	-30	10	Group	123	4.046	0.144
					Condition	123	0.002	0.968
					Group * Condition	123	0.928	0.766
BA 42L	Transverse temporal gyrus	-60	-10	15	Group	123	4.553	0.175
					Condition	123	0.005	0.983
					Group * Condition	123	2.367	0.635
BA 47L	Inferior frontal gyrus	-30	25	-15	Group	123	0.452	0.740
					Condition	123	0.024	1.000
					Group * Condition	123	12.537	**0.007***
BA 40L	Inferior parietal lobule	50	-30	45	Group	123	1.147	0.550
					Condition	123	4.236	0.525
					Group * Condition	123	0.673	0.796
BA 6R	Middle frontal gyrus	30	-5	55	Group	123	6.867	0.063
					Condition	123	0.020	1.000
					Group * Condition	123	1.622	0.732
BA 7R	Precuneus	15	-65	50	Group	123	0.225	0.837
					Condition	123	1.815	0.750
					Group * Condition	123	7.510	0.058
BA 9R	Middle frontal gyrus	30	30	35	Group	123	0.004	0.948
					Condition	123	0.081	1.000
					Group * Condition	123	0.601	0.786
BA 13R	Insula	35	15	-5	Group	123	0.215	0.804
					Condition	123	7.909	0.150
					Group * Condition	123	0.006	0.940
BA 17R	Lingual gyrus	15	-85	0	Group	123	0.243	0.865
					Condition	123	1.941	0.830
					Group * Condition	123	0.008	1.000

BA 41R	Superior temporal gyrus	55	-20	5	Group	123	1.735	0.475
					Condition	123	3.693	0.475
					Group * Condition	123	0.259	0.849
BA 24R	Anterior cingulate	5	30	20	Group	123	1.411	0.539
					Condition	123	0.014	1.000
					Group * Condition	123	2.323	0.542
BA 38R	Superior temporal gyrus	40	15	-30	Group	123	0.118	0.796
					Condition	123	1.392	0.667
					Group * Condition	123	1.081	0.753
BA 40R	Inferior parietal lobule	50	-45	45	Group	123	0.184	0.796
					Condition	123	1.744	0.675
					Group * Condition	123	0.587	0.742
BA 41R	Transverse temporal gyrus	45	-30	10	Group	123	0.817	0.575
					Condition	123	1.690	0.613
					Group * Condition	123	0.114	0.877
BA 42R	Transverse temporal gyrus	60	-10	15	Group	123	0.184	0.760
					Condition	123	0.666	0.867
					Group * Condition	123	0.006	0.975
BA 47R	Inferior frontal gyrus	30	25	-15	Group	123	0.050	0.858
					Condition	123	1.383	0.605
					Group * Condition	123	0.756	0.804

Abbreviation: MNI, Montreal Neurological Institute; FDR, false discovery rate; L, left; R, right.
a. Analysis of covariance with age and sex as covariates.
* FDR-corrected p value is at <0.05.
**FDR-corrected p value is at <0.005.

Bibliography

Ashinoff, B. K., & Abu-Akel, A. (2021). Hyperfocus: the forgotten frontier of attention. *Psychol Res*, *85*(1), 1-19. https://doi.org/10.1007/s00426-019-01245-8

Balz, J., Roa Romero, Y., Keil, J., Krebber, M., Niedeggen, M., Gallinat, J., & Senkowski, D. (2016). Beta/Gamma Oscillations and Event-Related Potentials Indicate Aberrant Multisensory Processing in Schizophrenia. *Front Psychol*, *7*, 1896. https://doi.org/10.3389/fpsyg.2016.01896

Barr, M. S., Rajji, T. K., Zomorrodi, R., Radhu, N., George, T. P., Blumberger, D. M., & Daskalakis, Z. J. (2017). Impaired theta-gamma coupling during working memory performance in schizophrenia. *Schizophr Res*, *189*, 104-110. https://doi.org/10.1016/j.schres.2017.01.044

Basar, E., & Guntekin, B. (2008). A review of brain oscillations in cognitive disorders and the role of neurotransmitters. *Brain Res*, *1235*, 172-193. https://doi.org/10.1016/j.brainres.2008.06.103

Basar, E., & Guntekin, B. (2013). Review of delta, theta, alpha, beta, and gamma response oscillations in neuropsychiatric disorders. *Suppl Clin Neurophysiol*, *62*, 303-341. https://doi.org/10.1016/b978-0-7020-5307-8.00019-3

Beck, V., Leonard, C., Robinson, B., Hahn, B., Hollingworth, A., Gold, J., & Luck, S. (2016). People with Schizophrenia Demonstrate More Optimal Feature-Guided Visual Search in a Probabilistic Search Task. *Journal of Vision*, *16*(12), 338-338. https://doi.org/10.1167/16.12.338

Bledowski, C., Prvulovic, D., Hoechstetter, K., Scherg, M., Wibral, M., Goebel, R., & Linden, D. E. (2004). Localizing P300 generators in visual target and distractor processing: a combined event-related potential and functional magnetic resonance imaging study. *J Neurosci*, *24*(42), 9353-9360. https://doi.org/10.1523/JNEUROSCI.1897-04.2004

Bowie, C. R., & Harvey, P. D. (2006). Cognitive deficits and functional outcome in schizophrenia. *Neuropsychiatr Dis Treat*, *2*(4), 531-536. https://doi.org/10.2147/nedt.2006.2.4.531

Brooks, H., Goodman, M. S., Bowie, C. R., Zomorrodi, R., Blumberger, D. M., Butters, M. A., Daskalakis, Z. J., Fischer, C. E., Flint, A., Herrmann, N., Kumar, S., Mah, L., Mulsant, B. H., Pollock, B. G., Voineskos, A. N., Rajji, T. K., & Group, P. A.-M. S. (2020). Theta-gamma coupling and ordering information: a stable brain-behavior relationship across cognitive tasks and clinical conditions. *Neuropsychopharmacology*, *45*(12), 2038-2047. https://doi.org/10.1038/s41386-020-0759-z

Canolty, R. T., Edwards, E., Dalal, S. S., Soltani, M., Nagarajan, S. S., Kirsch, H. E., Berger, M. S., Barbaro, N. M., & Knight, R. T. (2006). High Gamma Power Is Phase-Locked to Theta Oscillations in Human Neocortex. *Science*, *313*(5793), 1626-1628. https://doi.org/doi:10.1126/science.1128115

Canolty, R. T., & Knight, R. T. (2010). The functional role of cross-frequency

coupling. *Trends Cogn Sci*, *14*(11), 506-515. https://doi.org/10.1016/j.tics.2010.09.001

Chaumon, M., Bishop, D. V., & Busch, N. A. (2015). A practical guide to the selection of independent components of the electroencephalogram for artifact correction. *J Neurosci Methods*, *250*, 47-63. https://doi.org/10.1016/j.jneumeth.2015.02.025

Chavan, C. F., Mouthon, M., Draganski, B., van der Zwaag, W., & Spierer, L. (2015). Differential patterns of functional and structural plasticity within and between inferior frontal gyri support training-induced improvements in inhibitory control proficiency. *Hum Brain Mapp*, *36*(7), 2527-2543. https://doi.org/10.1002/hbm.22789

Colgin, L. L. (2015). Theta-gamma coupling in the entorhinal-hippocampal system. *Curr Opin Neurobiol*, *31*, 45-50. https://doi.org/10.1016/j.conb.2014.08.001

Daniel H. Mathalon, Ph.D., M.D. ,, Theda Heinks, Dipl.Psych. , and, & Judith M. Ford, Ph.D. (2004). Selective Attention in Schizophrenia: Sparing and Loss of Executive Control. *American Journal of Psychiatry*, *161*(5), 872-881. https://doi.org/10.1176/appi.ajp.161.5.872

Delorme, A., & Makeig, S. (2004). EEGLAB: an open source toolbox for analysis of single-trial EEG dynamics including independent component analysis. *J Neurosci Methods*, *134*(1), 9-21. https://doi.org/10.1016/j.jneumeth.2003.10.009

Duncan, E., Roach, B. J., Massa, N., Hamilton, H. K., Bachman, P. M., Belger, A., Carrion, R. E., Johannesen, J. K., Light, G. A., Niznikiewicz, M. A., Addington, J. M., Bearden, C. E., Cadenhead, K. S., Cannon, T. D., Cornblatt, B. A., McGlashan, T. H., Perkins, D. O., Tsuang, M., Walker, E. F., . . . Mathalon, D. H. (2022). Auditory N100 amplitude deficits predict conversion to psychosis in the North American Prodrome Longitudinal Study (NAPLS-2) cohort. *Schizophr Res*, *248*, 89-97. https://doi.org/10.1016/j.schres.2022.07.019

Fan, J., & Posner, M. (2004). Human attentional networks. *Psychiatr Prax*, *31 Suppl 2*, S210-214. https://doi.org/10.1055/s-2004-828484

Friston, K. J. (1998). The disconnection hypothesis. *Schizophr Res*, *30*(2), 115-125. https://doi.org/10.1016/s0920-9964(97)00140-0

Galaverna, F. S., Morra, C. A., & Bueno, A. M. (2012). Attention in patients with chronic schizophrenia: Deficit in inhibitory control and positive symptoms. *The European Journal of Psychiatry*, *26*, 185-195. http://scielo.isciii.es/scielo.php?script=sci_arttext&pid=S0213-61632012000300005&nrm=iso

Gold, J. M., Fuller, R. L., Robinson, B. M., McMahon, R. P., Braun, E. L., & Luck, S. J. (2006). Intact attentional control of working memory encoding in schizophrenia. *J Abnorm Psychol*, *115*(4), 658-673. https://doi.org/10.1037/0021-843X.115.4.658

Golubic, S. J., Jurasic, M. J., Susac, A., Huonker, R., Gotz, T., & Haueisen, J. (2019). Attention modulates topology and dynamics of auditory sensory gating. *Hum Brain Mapp*, *40*(10), 2981-2994. https://doi.org/10.1002/hbm.24573

Gur, R. E., & Gur, R. C. (2010). Functional magnetic resonance imaging in schizophrenia. *Dialogues Clin Neurosci*, *12*(3), 333-343. https://doi.org/10.31887/DCNS.2010.12.3/rgur

Haciahmet, C. C., Frings, C., & Pastotter, B. (2021). Target Amplification and Distractor Inhibition: Theta Oscillatory Dynamics of Selective Attention in a Flanker Task. *Cogn Affect Behav Neurosci*, *21*(2), 355-371. https://doi.org/10.3758/s13415-021-00876-y

Hahn, B., Bae, G. Y., Robinson, B. M., Leonard, C. J., Luck, S. J., & Gold, J. M. (2020). Cortical hyperactivation at low working memory load: A primary processing abnormality in people with schizophrenia? *Neuroimage Clin*, *26*, 102270. https://doi.org/10.1016/j.nicl.2020.102270

Hahn, B., Robinson, B. M., Kiat, J. E., Geng, J., Bansal, S., Luck, S. J., & Gold, J. M. (2022). Impaired Filtering and Hyperfocusing: Neural Evidence for Distinct Selective Attention Abnormalities in People with Schizophrenia. *Cereb Cortex*, *32*(9), 1950-1964. https://doi.org/10.1093/cercor/bhab327

Hamilton, H. K., Woods, S. W., Roach, B. J., Llerena, K., McGlashan, T. H., Srihari, V. H., Ford, J. M., & Mathalon, D. H. (2019). Auditory and Visual Oddball Stimulus Processing Deficits in Schizophrenia and the Psychosis Risk Syndrome: Forecasting Psychosis Risk With P300. *Schizophr Bull*, *45*(5), 1068-1080. https://doi.org/10.1093/schbul/sby167

Herrmann, C. S., Struber, D., Helfrich, R. F., & Engel, A. K. (2016). EEG oscillations: From correlation to causality. *Int J Psychophysiol*, *103*, 12-21. https://doi.org/10.1016/j.ijpsycho.2015.02.003

Hill, A. T., Hadas, I., Zomorrodi, R., Voineskos, D., Farzan, F., Fitzgerald, P. B., Blumberger, D. M., & Daskalakis, Z. J. (2020). Modulation of functional network properties in major depressive disorder following electroconvulsive therapy (ECT): a resting-state EEG analysis. *Sci Rep*, *10*(1), 17057. https://doi.org/10.1038/s41598-020-74103-y

Hirano, Y., & Uhlhaas, P. J. (2021). Current findings and perspectives on aberrant neural oscillations in schizophrenia. *Psychiatry Clin Neurosci*, *75*(12), 358-368. https://doi.org/10.1111/pcn.13300

Hsu, Y. F., Waszak, F., Strommer, J., & Hamalainen, J. A. (2021). Human Brain Ages With Hierarchy-Selective Attenuation of Prediction Errors. *Cereb Cortex*, *31*(4), 2156-2168. https://doi.org/10.1093/cercor/bhaa352

Javitt, D. C., Siegel, S. J., Spencer, K. M., Mathalon, D. H., Hong, L. E., Martinez, A., Ehlers, C. L., Abbas, A. I., Teichert, T., Lakatos, P., & Womelsdorf, T. (2020). A roadmap for development of neuro-oscillations as translational biomarkers for treatment development in neuropsychopharmacology. *Neuropsychopharmacology*, *45*(9), 1411-1422. https://doi.org/10.1038/s41386-020-0697-9

Kahn, R. S., & Keefe, R. S. (2013). Schizophrenia is a cognitive illness: time for a change in focus. *JAMA Psychiatry*, *70*(10), 1107-1112. https://doi.org/10.1001/jamapsychiatry.2013.155

Kiehl, K. A., & Liddle, P. F. (2001). An event-related functional magnetic resonance imaging study of an auditory oddball task in schizophrenia. *Schizophr Res*,

48(2-3), 159-171. https://doi.org/10.1016/s0920-9964(00)00117-1
Kim, H. (2014). Involvement of the dorsal and ventral attention networks in oddball stimulus processing: a meta-analysis. *Hum Brain Mapp*, *35*(5), 2265-2284. https://doi.org/10.1002/hbm.22326
Kim, M., Lee, T. H., Kim, J. H., Hong, H., Lee, T. Y., Lee, Y., Salisbury, D. F., & Kwon, J. S. (2018). Decomposing P300 into correlates of genetic risk and current symptoms in schizophrenia: An inter-trial variability analysis. *Schizophr Res*, *192*, 232-239. https://doi.org/10.1016/j.schres.2017.04.001
Kim, M., Lee, T. H., Park, H., Moon, S. Y., Lho, S. K., & Kwon, J. S. (2022). Thalamocortical dysrhythmia in patients with schizophrenia spectrum disorder and individuals at clinical high risk for psychosis. *Neuropsychopharmacology*, *47*(3), 673-680. https://doi.org/10.1038/s41386-021-01180-6
Lee, T. H., Kim, M., Hwang, W. J., Kim, T., Kwak, Y. B., & Kwon, J. S. (2020). Relationship between resting-state theta phase-gamma amplitude coupling and neurocognitive functioning in patients with first-episode psychosis. *Schizophr Res*, *216*, 154-160. https://doi.org/10.1016/j.schres.2019.12.010
Liakakis, G., Nickel, J., & Seitz, R. J. (2011). Diversity of the inferior frontal gyrus--a meta-analysis of neuroimaging studies. *Behav Brain Res*, *225*(1), 341-347. https://doi.org/10.1016/j.bbr.2011.06.022
Lisman, J., & Buzsaki, G. (2008). A neural coding scheme formed by the combined function of gamma and theta oscillations. *Schizophr Bull*, *34*(5), 974-980. https://doi.org/10.1093/schbul/sbn060
Lisman, J. E., & Jensen, O. (2013). The theta-gamma neural code. *Neuron*, *77*(6), 1002-1016. https://doi.org/10.1016/j.neuron.2013.03.007
Luck, S. J., Hahn, B., Leonard, C. J., & Gold, J. M. (2019). The Hyperfocusing Hypothesis: A New Account of Cognitive Dysfunction in Schizophrenia. *Schizophr Bull*, *45*(5), 991-1000. https://doi.org/10.1093/schbul/sbz063
Luck, S. J., McClenon, C., Beck, V. M., Hollingworth, A., Leonard, C. J., Hahn, B., Robinson, B. M., & Gold, J. M. (2014). Hyperfocusing in schizophrenia: Evidence from interactions between working memory and eye movements. *J Abnorm Psychol*, *123*(4), 783-795. https://doi.org/10.1037/abn0000003
Lynn, P. A., & Sponheim, S. R. (2016). Disturbed theta and gamma coupling as a potential mechanism for visuospatial working memory dysfunction in people with schizophrenia. *Neuropsychiatric Electrophysiology*, *2*(1). https://doi.org/10.1186/s40810-016-0022-3
Mathalon, D. H., & Sohal, V. S. (2015). Neural Oscillations and Synchrony in Brain Dysfunction and Neuropsychiatric Disorders: It's About Time. *JAMA Psychiatry*, *72*(8), 840-844. https://doi.org/10.1001/jamapsychiatry.2015.0483
Minzenberg, M. J., Firl, A. J., Yoon, J. H., Gomes, G. C., Reinking, C., & Carter, C. S. (2010). Gamma oscillatory power is impaired during cognitive control independent of medication status in first-episode schizophrenia. *Neuropsychopharmacology*, *35*(13), 2590-2599. https://doi.org/10.1038/npp.2010.150

Mueller, E. M., Makeig, S., Stemmler, G., Hennig, J., & Wacker, J. (2011). Dopamine effects on human error processing depend on catechol-O-methyltransferase VAL158MET genotype. *J Neurosci*, *31*(44), 15818-15825. https://doi.org/10.1523/JNEUROSCI.2103-11.2011

Mwansisya, T. E., Hu, A., Li, Y., Chen, X., Wu, G., Huang, X., Lv, D., Li, Z., Liu, C., Xue, Z., Feng, J., & Liu, Z. (2017). Task and resting-state fMRI studies in first-episode schizophrenia: A systematic review. *Schizophr Res*, *189*, 9-18. https://doi.org/10.1016/j.schres.2017.02.026

Palva, J. M., Palva, S., & Kaila, K. (2005). Phase synchrony among neuronal oscillations in the human cortex. *J Neurosci*, *25*(15), 3962-3972. https://doi.org/10.1523/JNEUROSCI.4250-04.2005

Papaioannou, O., Crespo, L. P., Clark, K., Ogbuagu, N. N., Alliende, L. M., Silverstein, S. M., & Erickson, M. A. (2022). Is Cortical Theta-Gamma Phase-Amplitude Coupling Memory-Specific? *Brain Sci*, *12*(9). https://doi.org/10.3390/brainsci12091131

Park, J. Y., Jhung, K., Lee, J., & An, S. K. (2013). Theta-gamma coupling during a working memory task as compared to a simple vigilance task. *Neurosci Lett*, *532*, 39-43. https://doi.org/10.1016/j.neulet.2012.10.061

Pascual-Marqui, R. D. (2002). Standardized low-resolution brain electromagnetic tomography (sLORETA): technical details. *Methods Find Exp Clin Pharmacol*, *24 Suppl D*, 5-12.

Popov, T., Wienbruch, C., Meissner, S., Miller, G. A., & Rockstroh, B. (2015). A mechanism of deficient interregional neural communication in schizophrenia. *Psychophysiology*, *52*(5), 648-656. https://doi.org/10.1111/psyp.12393

Rajji, T. K., Zomorrodi, R., Barr, M. S., Blumberger, D. M., Mulsant, B. H., & Daskalakis, Z. J. (2017). Ordering Information in Working Memory and Modulation of Gamma by Theta Oscillations in Humans. *Cereb Cortex*, *27*(2), 1482-1490. https://doi.org/10.1093/cercor/bhv326

Riddle, J., Vogelsang, D. A., Hwang, K., Cellier, D., & D'Esposito, M. (2020). Distinct Oscillatory Dynamics Underlie Different Components of Hierarchical Cognitive Control. *J Neurosci*, *40*(25), 4945-4953. https://doi.org/10.1523/JNEUROSCI.0617-20.2020

Rosburg, T., Marinou, V., Haueisen, J., Smesny, S., & Sauer, H. (2004). Effects of lorazepam on the neuromagnetic mismatch negativity (MMNm) and auditory evoked field component N100m. *Neuropsychopharmacology*, *29*(9), 1723-1733. https://doi.org/10.1038/sj.npp.1300477

Sawaki, R., Kreither, J., Leonard, C. J., Kaiser, S. T., Hahn, B., Gold, J. M., & Luck, S. J. (2017). Hyperfocusing of attention on goal-related information in schizophrenia: Evidence from electrophysiology. *J Abnorm Psychol*, *126*(1), 106-116. https://doi.org/10.1037/abn0000209

Schroger, E., Marzecova, A., & SanMiguel, I. (2015). Attention and prediction in human audition: a lesson from cognitive psychophysiology. *Eur J Neurosci*, *41*(5), 641-664. https://doi.org/10.1111/ejn.12816

Sheffield, J. M., & Barch, D. M. (2016). Cognition and resting-state functional connectivity in schizophrenia. *Neurosci Biobehav Rev*, *61*, 108-120.

https://doi.org/10.1016/j.neubiorev.2015.12.007
Shim, M., Kim, D. W., Lee, S. H., & Im, C. H. (2014). Disruptions in small-world cortical functional connectivity network during an auditory oddball paradigm task in patients with schizophrenia. *Schizophr Res*, *156*(2-3), 197-203. https://doi.org/10.1016/j.schres.2014.04.012
Shin, Y. W., O'Donnell, B. F., Youn, S., & Kwon, J. S. (2011). Gamma oscillation in schizophrenia. *Psychiatry Investig*, *8*(4), 288-296. https://doi.org/10.4306/pi.2011.8.4.288
Sohrabpour, A., Lu, Y., Kankirawatana, P., Blount, J., Kim, H., & He, B. (2015). Effect of EEG electrode number on epileptic source localization in pediatric patients. *Clin Neurophysiol*, *126*(3), 472-480. https://doi.org/10.1016/j.clinph.2014.05.038
Tort, A. B., Komorowski, R., Eichenbaum, H., & Kopell, N. (2010). Measuring phase-amplitude coupling between neuronal oscillations of different frequencies. *J Neurophysiol*, *104*(2), 1195-1210. https://doi.org/10.1152/jn.00106.2010
Ueoka, Y., Tomotake, M., Tanaka, T., Kaneda, Y., Taniguchi, K., Nakataki, M., Numata, S., Tayoshi, S., Yamauchi, K., Sumitani, S., Ohmori, T., Ueno, S., & Ohmori, T. (2011). Quality of life and cognitive dysfunction in people with schizophrenia. *Prog Neuropsychopharmacol Biol Psychiatry*, *35*(1), 53-59. https://doi.org/10.1016/j.pnpbp.2010.08.018
Uhlhaas, P. J., Haenschel, C., Nikolic, D., & Singer, W. (2008). The role of oscillations and synchrony in cortical networks and their putative relevance for the pathophysiology of schizophrenia. *Schizophr Bull*, *34*(5), 927-943. https://doi.org/10.1093/schbul/sbn062
Uhlhaas, P. J., & Singer, W. (2010). Abnormal neural oscillations and synchrony in schizophrenia. *Nat Rev Neurosci*, *11*(2), 100-113. https://doi.org/10.1038/nrn2774
Voytek, B., D'Esposito, M., Crone, N., & Knight, R. T. (2013). A method for event-related phase/amplitude coupling. *Neuroimage*, *64*, 416-424. https://doi.org/10.1016/j.neuroimage.2012.09.023
Wang, R., Liu, M., Cheng, X., Wu, Y., Hildebrandt, A., & Zhou, C. (2021). Segregation, integration, and balance of large-scale resting brain networks configure different cognitive abilities. *Proc Natl Acad Sci U S A*, *118*(23). https://doi.org/10.1073/pnas.2022288118

Abstract in Korean

배경: 선택적 주의력은 조현병 환자의 인지 증상의 기저가 될 수 있는 중요한 인지 기능이다. 뇌 진동의 손상은 이러한 인지 손상에 기여할 수 있으며, 특히 세타 위상-감마 진폭 결합은 감각 정보 처리, 주의력, 작업 기억에 중요한 역할을 한다는 사실이 밝혀졌다. 이번 연구에서는 세타 위상-감마 진폭 연결성을 사용하여 조현병 환자의 주의력 손상을 설명하는 새로운 접근인 비정상적인 과집중에 대한 뇌파 마커를 조사하고자 한다.

방법: 54명의 조현병 환자와 73명의 건강 대조군에게서 청각 오드볼 과제를 수행하는 동안 뇌파를 측정하였다. 비표적 조건과 표적 조건 각각에 대해 주의력 네트워크와 감각 정보 처리와 관련된 25개의 뇌 영역의 신호를 사용하여 세타-감마 연결성을 계산하였고, 이원 혼합 공분산 분석을 통해 집단 간 비교하였다. 또한 변화된 세타-감마 연결성과 선로 잇기 검사 (Trail Making Test) 유형 A와 B 사이의 상관 분석을 확인하였다.

결과: 비표적 조건에서 조현병 환자는 정상 대조군과 비교하여 좌측 아래이마이랑 및 관자이랑의 세타-감마 연결성이 유의하게 높았지만, 표적 조건에서는 차이가 없음이 확인되었다. 조현병 환자에서 좌측 아래이마이랑의 세타-감마 연결성 증가는 선로 잇기 검사 파트 A 및 파트 B의 처리 속도와 양적 상관관계가 확인되었다.

결론: 주의력 관련 영역에서 조현병의 세타-감마 연결성 상승은 비정상적인 과집중을 나타내며, 이는 선로 잇기 검사 유형 A와 B 모두에서 상관이 확인되었다. 이는 세타-감마 연결성이 조현병 환자의 인지 증상을 초래할 수 있는 비정상적인 과집중에 대한 전기 생리학적 마커가 될 수 있음을 시사한다.